Available online at www.sciencedirect.com

Journal of Catalysis 214 (2003) 130–135

JOURNAL OF CATALYSIS

www.elsevier.com/locate/jcat

The reaction pathway and kinetic mechanism of the catalytic oxidation of gaseous lean TCE on Pd/alumina catalysts

A. Aranzabal, J.L. Ayastuy-Arizti, J.A. González-Marcos, and J.R. González-Velasco *

Department of Chemical Engineering, Faculty of Sciences, Universidad del País Vasco/EHU, PO Box 644, E-48080 Bilbao, Spain

Received 12 June 2002; revised 22 October 2002; accepted 4 November 2002

Abstract

The complete catalytic oxidation of trichloroethylene (TCE) over palladium supported on alumina was evaluated. The effect of temperature, inlet TCE concentration, and the space time on the reaction rate and selectivity was examined with the aim of better understanding of the reaction pathway. TCE oxidation reactions were carried out in a conventional fixed-bed reactor at atmospheric pressure under conditions of lean TCE concentration (600–1300 ppm) in air, between 150 and 550 °C; space time was varied between 1100 and 3500 $\mathrm{kg\,s\,mol_{TCE}}^{-1}$. The outlet composition was analyzed by a gas chromatograph, equipped with an electron capture detector (ECD) and a thermal conductivity detector (TCD). The product (CO, CO_2, C_2Cl_4, HCl, and Cl_2) distribution kinetic data were used to formulate a set of reaction rate equations that account for a five-reaction network. The kinetic model, based on an Eley–Rideal type of mechanism, correlated kinetic data.

Keywords: Catalytic oxidation; Selectivity; Trichloroethylene; Noble metal catalysts; Palladium; Kinetics; Mechanisms; VOC

1. Introduction

Emissions of chlorinated volatile organic compounds (CVOC) constitute a major source of atmospheric pollution by contributing to photochemical smog formation and depletion of the ozone layer in the stratosphere. Catalytic oxidation of CVOC is currently receiving increased attention because of its energetic and efficiency advantages in meeting increasingly stringent environmental regulations.

In designing a catalyst and a reactor for an end-of-pipe environmental control system, such as CVOC abatement, both high activity and high selectivity toward environmentally desirable products (CO_2, H_2O, and HCl), minimizing formation of potentially toxic by-products, are required. Because of this, the formation of by-products must be carefully studied. Such work has already been done and reported in two previous papers [1,2] by analyzing the activity and product distribution in CVOC oxidation catalyzed by Pd and Pt on γ-alumina. The 0.44 wt.% Pt/Al_2O_3 and 0.42 wt.% Pd/Al_2O_3 catalysts were highly active for deep oxidation of TCE, that was completely destroyed at 550 °C. The palladium catalysts were more active than the platinum catalysts, advancing the light-off curves 40 °C for TCE oxidation. The Pt catalyst was fully selective to CO_2, while CO was detected over Pd catalysts, presenting two peak concentrations at 400 and 550 °C, respectively. The oxidation of TCE produced a notable amount of C_2Cl_4, less with platinum than with palladium, together with HCl and Cl_2. The concentration of C_2Cl_4 peaked at 450 °C and was reduced to practically zero at 550 °C, as its oxidation rate increased above its formation rate.

Selectivity to hydrogen chloride was much improved with the addition of hydrogen-supplying compounds (water, hexane, and toluene) to the feedstream by removing chlorine attached to the catalyst surface [2]. Increasing water concentration resulted in lower selectivity to Cl_2 and C_2Cl_4. In the presence of water, complete oxidation of CO was promoted by the water-shift reaction, resulting in 100% selectivity to CO_2.

The proper design of a reactor for catalytic oxidation requires knowledge of kinetic and transport parameters and appropriate mathematical description of the reactor behavior under realistic conditions, usually a mass-transfer-controlled regime. In any case, the ignition temperature of the reactor, a parameter of great importance for controlling the process, is dependent on kinetics.

---

* Corresponding author.
E-mail address: iqpgovej@lg.ehu.es (J.R. González-Velasco).

0021-9517/03/$ – see front matter © 2003 Elsevier Science (USA). All rights reserved.
doi:10.1016/S0021-9517(02)00091-X

The literature involving kinetic rate expressions for the oxidation of chlorinated volatile organic compounds over platinum and palladium catalysts is rather limited. The reaction mechanism is believed to involve a reaction between adsorbed oxygen and an adsorbed reactant molecule (Langmuir–Hinshelwood mechanism) [3–5] or a reaction between adsorbed oxygen and a gas-phase reactant molecule (Eley–Rideal mechanism) [6–8]. Both of these assumptions have been used in the development of kinetic rate expressions to describe the oxidative conversion of chlorinated volatile organic compound over supported noble metal catalysts. However, selectivity data have not been considered, limiting the applicability of the kinetic models reported in the literature. Rossin and co-workers [3–5] took into account the inhibition effect of the product HCl (assuming that all chlorine atoms were converted to HCl) by adding a product inhibition term to the reaction rate expression.

Carrying on with the research reported in the two previous papers [1,2], the objective of this work is to experimentally determine the global kinetics for TCE oxidation that could describe both the oxidation rate of CVOC and the product formation rate in order to predict the final effluent composition. TCE was chosen as a suitable model compound present in many off-gases, such as groundwater stripping emissions and dry cleaning and degreasing processes [9]. Our approach to meeting the stated objective was to examine the effect of temperature, space velocity, and inlet concentration on the reaction rate and selectivity with the aim of a better understanding of the reaction pathway.

2. Experimental

SCM-129X γ-alumina spheres supplied by Rhône–Poulenc were calcined in air at 700 °C for 4 h and then crushed and sieved to the desired particle size. Characterization led to the following properties: BET surface area, 114 $m^2\,g^{-1}$; pore volume, 0.5 $cm^3\,g^{-1}$; average pore radius, 8.7 nm; predominant pore radius, 8.6 nm; isoelectric point, 9.

The active phase Pd was incorporated by adsorption of $PdCl_2$ from aqueous solution using 40 cm^3 of solution per gram of alumina. The nominal composition of the prepared catalyst was 0.5 wt.%. After drying for 1 h at 150 °C, final activation of the precursor was made by calcining at 550 °C in an air stream for 4 h and reducing at 550 °C in an $N_2/H_2 = 3/1$ stream for an additional 2 h. The final catalysts resulted in 0.42 wt.% Pd, measured by atomic absorption spectroscopy (AAS); the metal dispersion was determined by hydrogen chemisorption to be 43%.

Oxidation reactions were carried out in a conventional fixed-bed flow reactor under atmospheric pressure. It consisted of a 12-mm i.d. stainless steel tube located inside an electrical furnace. In the lower part of the reactor, the catalyst was placed on a plug of glass wool. In order to preheat the gas feedstream, crushed quartz glass (10 cm^3, 2 mm o.d.) was placed above the catalyst bed. The temperature at the inlet was automatically controlled with a K-type thermocouple. The oxidation reaction was carried out under thermal combustion conditions by placing just 0.3–0.5 mm of crushed quartz glass in the reactor.

The feedstream to the reactor was prepared by delivering the liquid TCE with a syringe pump into dry, oil-free compressed air, which was purified using a commercial PSA drier and metered by a mass flow controller. The injection point was electrically heated to ensure complete evaporation. Before entering the reactor, the feedstream went through a 2-dm^3 static mixer to dampen out possible concentration oscillations associated with the running of the syringe pump. The flow rate through the reactor was set at 0.12 $m\,s^{-1}$; thus different TCE feed concentrations and residence times were achieved by changing the syringe pump flow and the catalyst weight.

A portion of the effluent stream was analyzed on line by a Hewlett Packard 5890 Series II gas chromatograph equipped with an electron capture detector (ECD) and a thermal conductivity detector (TCD). CO and CO_2 were separated by both a 13X molecular sieve column and a Hayesep N column interconnected to a gas sampling loop by a single 10-port valve and were analyzed on the TCD. The concentration of TCE, as well as any other chlorinated hydrocarbons formed in the reaction, was determined on the ECD after separation in an HP-VOC column. Analysis of both Cl_2 and HCl was performed by bubbling the effluent stream through a 0.0125 N NaOH solution [10]. Then Cl_2 concentration was determined by titration with ferrous ammonium sulphate (FAS) using *N*,*N*-diethyl-*p*-phenylenediamine (DPD) as indicator [11]. The concentration of chloride ions in the bubbled solution was determined using an ion selective electrode.

3. Results and discussion

3.1. Transport effects

Mass transfer effects were evaluated to ensure that kinetic experiments were carried out under conditions free of diffusional resistances. Results are discussed elsewhere [1].

3.2. Effect of temperature

The effect of temperature on TCE catalytic oxidation over 0.42% Pd/Al_2O_3 has been investigated in previous works [1,2]. According to the product distribution profiles (Fig. 1), a reaction mechanism was proposed for TCE destruction:

$$C_2HCl_3 + xO_2 \rightarrow 2CO_x + HCl + Cl_2, \quad x = 1, 2, \tag{1}$$

$$C_2HCl_3 + Cl_2 \rightarrow (CCl_3\text{–}CHCl_2) \rightarrow C_2Cl_4 + HCl, \tag{2}$$

$$CO + \tfrac{1}{2}O_2 \rightarrow CO_2, \tag{3}$$

$$C_2Cl_4 + 2O_2 \rightarrow 2CO_2 + 2Cl_2. \tag{4}$$

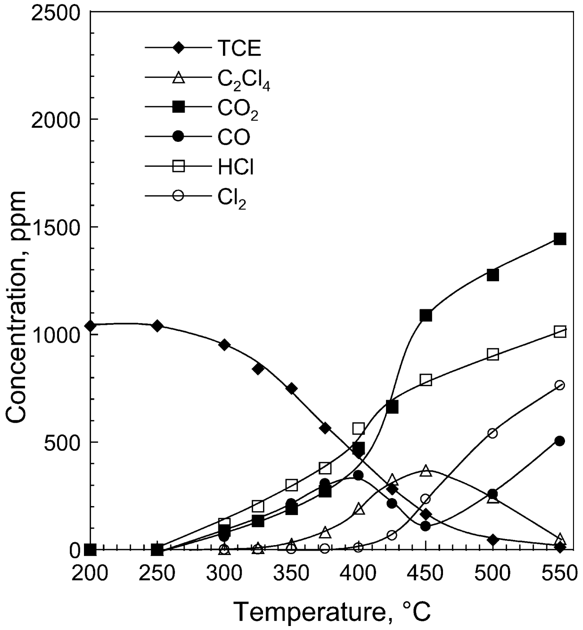

Fig. 1. Product distribution profiles in the oxidation of TCE over 0.42% Pd/Al_2O_3 as a function of temperature.

The formation of Cl_2 by the Deacon reaction can also be expected due to the high oxygen concentration in the reaction environment [2]:

$$2HCl + \tfrac{1}{2}O_2 \rightleftharpoons H_2O + Cl_2. \qquad (5)$$

3.3. Effect of residence time

The presence of both CO and CO_2 within the products can be explained by two reaction schemes: as parallel reactions,

$$C_2HCl_3 + 2O_2 \rightarrow 2CO_2 + HCl + Cl_2, \qquad (6)$$

$$C_2HCl_3 + O_2 \rightarrow 2CO + HCl + Cl_2, \qquad (7)$$

or as series reactions,

$$C_2HCl_3 + O_2 \rightarrow 2CO + HCl + Cl_2, \qquad (7)$$

$$CO + \tfrac{1}{2}O_2 \rightarrow CO_2. \qquad (3)$$

Experiments with variable residence time were carried out to find whether TCE oxidative decomposition happens via the above-mentioned series or parallel reaction mechanisms, reactions (6), (7), and (3). Figure 2 shows selectivity to CO during TCE oxidation as a function of residence time at three different temperatures. Higher temperatures were not included because CO oxidation becomes very fast above 350 °C.

It can be noticed that selectivity for CO remained practically constant over the whole range of residence times. If the formation of CO_2 were due to the oxidation of CO (suggesting a series reaction) then when the residence time decreased the selectivity of the catalyst to the formation of CO_2 should decrease, and vice versa for the formation of CO. It can be seen clearly that this is not the case. Conversely, if the formation of CO and CO_2 occurred from parallel reactions, any variation in residence time would not be expected to affect the selectivity of the catalyst toward the formation of these products. This behavior is observed in Fig. 2. Ramanathan et al. [12] also observed a reaction mechanism for the oxidation of methylene chloride with two parallel oxidations.

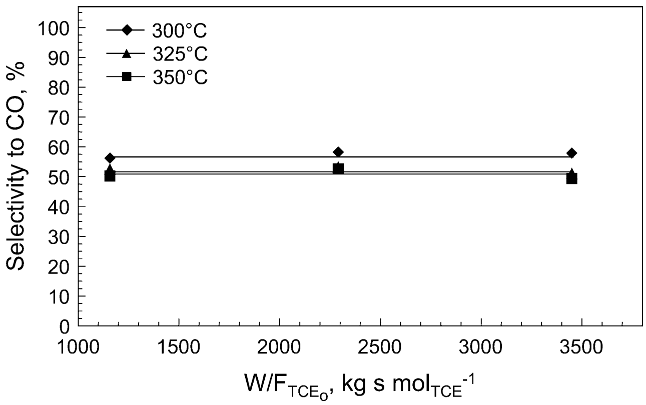

Fig. 2. Selectivity to CO as a function of space time in the oxidation of 1040-ppm TCE.

Fig. 3 shows the conversion of TCE as a function of residence time at different temperatures. As expected, the conversion increased with residence time, indicating that the kinetic equation for the oxidative rate is a function of the TCE partial pressure.

3.4. Influence of inlet TCE concentration

In order to explore the relationship between the oxidative rate and TCE partial pressure, conversion was plotted as a function of the inlet concentration of TCE. A set of experiments with different TCE feed concentrations were carried out, keeping constant the residence time of 2290 kg s mol_{TCE}^{-1}. Conversion was recorded within the range of temperatures from 300 to 400 °C (Fig. 4). The increase of

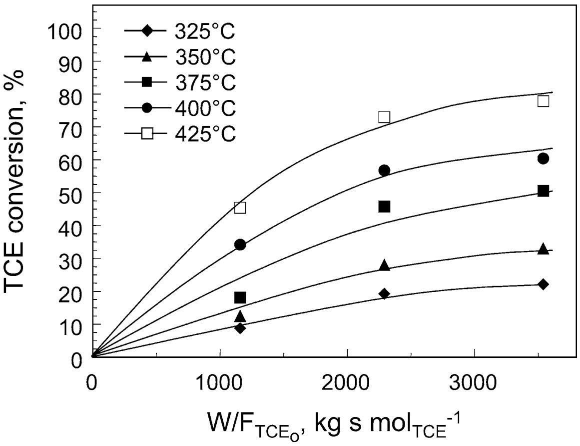

Fig. 3. Conversion of 1040-ppm TCE as a function of space time and temperature.

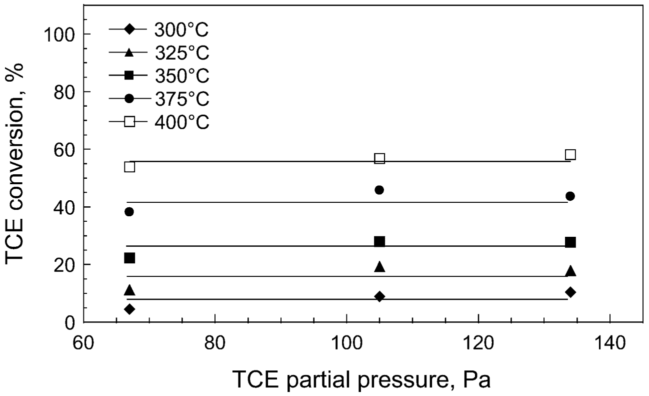

Fig. 4. Conversion of TCE as a function of feed concentration and temperature at 2290 kg s $\mathrm{mol_{TCE}}^{-1}$.

the inlet concentration from 690 to 1200 ppm practically did not affect the conversion, suggesting a first-order reaction for TCE. This conclusion can be easily derived by integrating the design equation of a fixed bed flow reactor,

$$\frac{W}{F_{\mathrm{TCE_0}}} = \int_0^X \frac{\mathrm{d}x_{\mathrm{TCE}}}{-r_{\mathrm{TCE}}} = \int_0^X \frac{\mathrm{d}x_{\mathrm{TCE}}}{kp_{\mathrm{TCE}}}, \tag{8}$$

which gives

$$x_{\mathrm{TCE}} = 1 - \exp\left[-k\left(\frac{W}{F_{\mathrm{TOT(in)}}} P_{\mathrm{TOT}}\right)\right]. \tag{9}$$

Eq. (9) means that if the total pressure (P_{TOT}) and therefore the total molar flow (F_{TOT}) are held constant, the conversion of TCE is independent of its concentration at the reactor inlet, as shown in Fig. 4.

Likewise, selectivity toward CO and CO_2 as a function of TCE inlet concentration showed a constant relationship (Fig. 5), indicating that both parallel oxidation reactions (partial and total oxidation) were first-order TCE dependent. Selectivity to CO and CO_2 in Fig. 5 was calculated considering all carbon-containing products (CO, CO_2, and C_2Cl_4) as follows:

$$S_{\mathrm{CO}} = \frac{[\mathrm{CO}]}{[\mathrm{CO}] + [\mathrm{CO_2}] + 2[\mathrm{C_2Cl_4}]} \times 100, \tag{10}$$

$$S_{\mathrm{CO_2}} = \frac{[\mathrm{CO_2}]}{[\mathrm{CO}] + [\mathrm{CO_2}] + 2[\mathrm{C_2Cl_4}]} \times 100. \tag{11}$$

Therefore, it could be concluded that chlorination of feed TCE to C_2Cl_4 was also a first-order reaction with respect to TCE. The set of reactions (6), (7), and (2) constitute the overall TCE decomposition, which must be a first-order reaction, since if the reaction order of any of these reactions were different from one, the overall decomposition would not be a first-order reaction and would not be consistent with the results in Figs. 4 and 5.

3.5. *Effect of oxygen concentration*

Very often, the effect of oxygen concentration is not evaluated in the catalytic oxidation of VOC, since the reaction is carried out under an excess of oxygen. However, the effect of oxygen concentration could provide useful information for discriminating between different mechanistic assumptions. In principle, a reaction between adsorbed TCE and oxygen can be assumed. Such a mechanism would result in lowering TCE conversion as oxygen concentration was increased. This clearly is not the case, since the results presented in Fig. 6 indicate that the reaction is independent of the oxygen concentration. Thus, the above mechanism must be excluded. Considering a reaction between adsorbed TCE and gas-phase oxygen, the reaction kinetics would be first-order with respect to oxygen concentration, which is inconsistent with data presented in Fig. 6. Furthermore, the TCE reaction order would be lower than one, since the kinetic equation would have an extra term in the denominator taking into account the adsorption of TCE onto the reactive sites, which also is inconsistent with results in Fig. 5.

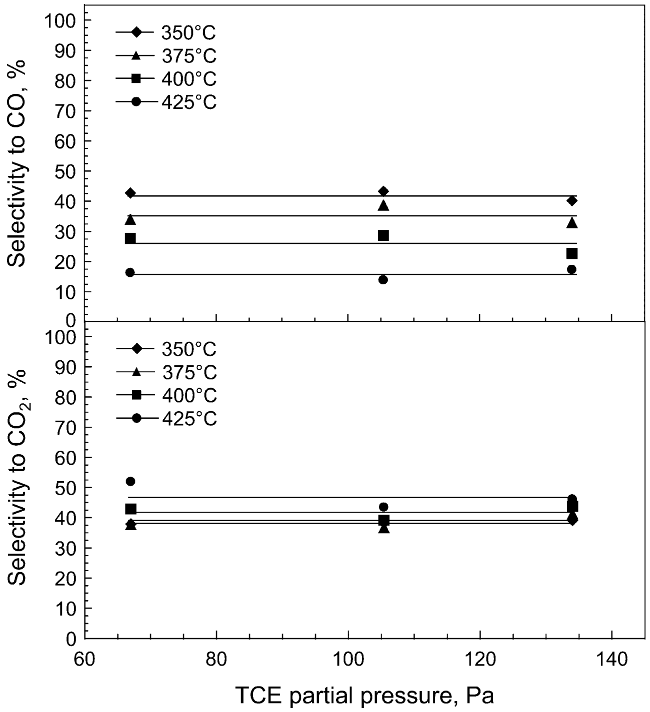

Fig. 5. Selectivity to CO and CO_2 as a function of TCE inlet concentration at 2290 kg s $\mathrm{mol_{TCE}}^{-1}$.

A reaction of TCE from the gas phase or by weak adsorption with chemisorbed oxygen covering the catalyst surface (Eley–Rideal mechanism) would lead to a first-order reaction with respect to TCE and a zero order reaction with respect to oxygen. Since oxygen is fed in excess, its concentration hardly changes, and therefore the term of oxygen concentration in the numerator and denominator (assuming a Langmuir–Hinshelwood equation) would keep constant. This mechanistic assumption agreed with the results in Fig. 6 and those reported by other authors in the oxidation of chlorinated VOC [4–8,13,14] and nonchlorinated VOC [15–19] over supported Pt and Pd catalysts.

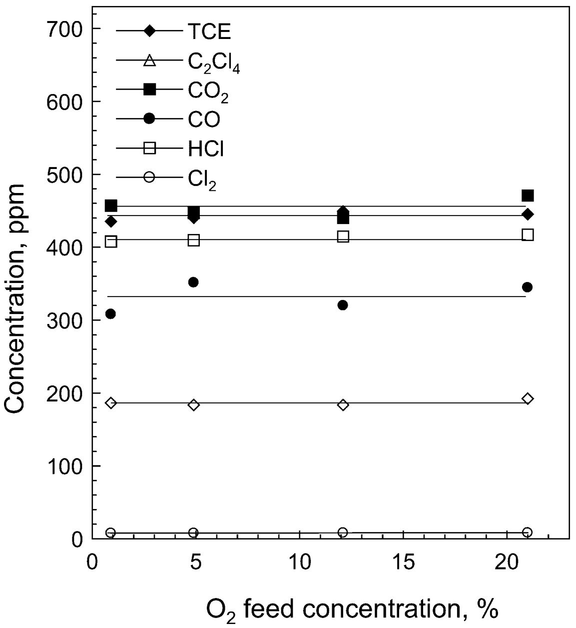

Fig. 6. Product distribution as a function of oxygen feed concentration in the oxidation of 1040 ppm at 300 °C and 2290 $\mathrm{kg\,s\,mol_{TCE}}^{-1}$.

On the basis of this work and consistent with the above referenced studies, the zero-order oxygen dependency was attributed to the catalyst surface being saturated with dissociatively adsorbed oxygen,

$$O_2 + (\ ) \rightarrow (O_2) \xrightarrow{\text{fast}} 2(O), \tag{12}$$

where ( ) and (O) represent reduced and oxidized sites, respectively. The adsorption step is relatively slow in comparison with molecular oxygen dissociation. Therefore, the adsorbed molecular oxygen concentration is negligible [18]. Dissociative chemisorption is followed by direct reaction of the gaseous TCE with (O), or the reactant may be weakly adsorbed first. Both Golodets [18] and Germain [20,21] have proposed that oxidation often occurs by a parallel–series mechanism. According to the redox mechanism [18], during the reaction the oxidized center retrieves the reduced state (12), and subsequently is quickly oxidized. That is, neither reactant nor products can appreciably compete with oxygen for reduced sites on the catalysts. Consequently, C_2Cl_4 and CO oxidation reactions are also zero-order oxygen-dependent, and therefore the concentration of these intermediate products is independent of oxygen concentration.

3.6. Reaction scheme and mechanism

The kinetic results discussed above and their conclusions make it possible to specify the global mechanism of the TCE oxidation reaction, consisting of the following five steps. The Deacon reaction (5) should also be considered, since under the studied conditions, it is very probable that HCl reacts with oxygen:

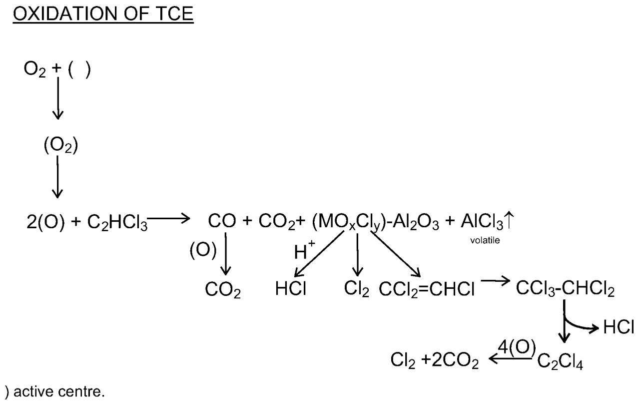

Fig. 7. Reaction pathway of TCE catalytic oxidation.

$$C_2HCl_3 + 2O_2 \rightarrow 2CO_2 + HCl + Cl_2, \tag{6}$$

$$C_2HCl_3 + O_2 \rightarrow 2CO + HCl + Cl_2, \tag{7}$$

$$C_2HCl_3 + Cl_2 \rightarrow (CCl_3\text{–}CHCl_2) \rightarrow C_2Cl_4 + HCl, \tag{2}$$

$$CO + \tfrac{1}{2}O_2 \rightarrow CO_2, \tag{3}$$

$$C_2Cl_4 + 2O_2 \rightarrow 2CO_2 + 2Cl_2, \tag{4}$$

$$2HCl + \tfrac{1}{2}O_2 \rightleftharpoons H_2O + Cl_2. \tag{5}$$

Fig. 7 shows schematically the conclusions arising from the above-discussed kinetic results along with those from previous works [2]. Oxygen is dissociatively adsorbed onto active centers. The dissociation step occurs very quickly in comparison with the adsorption step, resulting in the full coverage of the active surface with atomic oxygen. Consequently gaseous TCE reacts directly with adsorbed oxygen, leading to CO and CO_2, according to Eley–Rideal mechanism. The oxidative decomposition of TCE involves C–Cl bond dissociation by chemical interaction of the halogen with the precious metal and the support, resulting in precious metal (oxide)–chloride species, $[M(O_x)Cl_y]$, on alumina and aluminum chloride. The metal (oxide)–chloride species can directly decompose to molecular chlorine (Cl_2) and also react with the feed TCE by transferring chlorine (Cl_2) to the double bond. The intermediate pentachloroethane is spontaneously dehydrochlorinated by HCl elimination, resulting in the more stable tetrachloroethylene. CO and C_2Cl_4 are also assumed to react from the gaseous phase with adsorbed atomic oxygen, as an Eley–Rideal mechanism. This reaction is promoted at higher temperatures, reducing their concentration at the reactor exit.

4. Conclusions

In this paper the reaction pathway of lean TCE oxidation on a granulated Pd/Al_2O_3 catalyst has been determined for a wide range of temperature, space velocity, and inlet concentration conditions. The analysis of product distribution at the reactor exit showed that CO and C_2Cl_4 were formed in the reaction. The reaction was therefore modeled by a five-step reaction—this being the minimum number of steps required to adequately account for byproduct formation.

The surface reaction mechanisms correspond to a single-site Eley–Rideal type of mechanism with the TCE molecule reacting from the gas phase with chemisorbed oxygen covering the catalyst surface. TCE is oxidized simultaneously to CO_2 and CO, leading to precious metal (oxide)–chloride species, which react with gas-phase feed TCE to produce C_2Cl_4. Oxidation of both CO and C_2Cl_4, effective as temperature increased, occurs also by interaction with chemisorbed oxygen from the gas phase.

Acknowledgments

The authors thank the Universidad del País Vasco/EHU (9/UPV-13517/2001) and the Ministerio de Educación y Cultura (PPQ2001-0543) for financial support.

References

[1] J.R. González-Velasco, A. Aranzabal, J.I. Gutiérrez Ortiz, R. López-Fonseca, M.A. Gutiérrez-Ortiz, Appl. Catal. B 19 (1998) 189.
[2] J.R. González-Velasco, A. Aranzabal, R. López-Fonseca, R. Ferret, J.A. González Marcos, Appl. Catal. B 24 (2000) 33.
[3] A.A. Klinghoffer, J.A. Rossin, Ind. Eng. Chem. Res. 31 (1992) 481.
[4] J.A. Rossin, M.M. Farris, Ind. Eng. Chem. Res. 32 (1993) 1024.
[5] D.M. Papenmeier, J.A. Rossin, Ind. Eng. Chem. Res. 33 (1994) 3094.
[6] Y. Wang, H. Shaw, R.J. Farrauto, Catalytic Control of Air Pollution, Mobile and Stationary Sources, in: ACS Symp. Ser., Vol. 495, Am. Chem. Society, Washington, DC, 1992, p. 125.
[7] T.-Ch. Yu, H. Shaw, R.J. Farrauto, Catalytic Control of Air Pollution, Mobile and Stationary Sources, in: ACS Symp. Ser., Vol. 495, Am. Chem. Society, Washington, DC, 1992, p. 141.
[8] J.C. Lou, S.S. Lee, Appl. Catal. B 12 (1997) 111.
[9] T.D. Hylton, Environ. Prog. 11 (1992) 54.
[10] Guía para la valoración de la contaminación del aire, in: Colección Senda Ambiental, Vol. 2, Ministerio de Sanidad y Consumo, Madrid, 1985 [In Spanish].
[11] A.E. Greenberg, L.S. Clesceri, A.D. Eaton (Eds.), Standard Methods for the Examination of Water and Wastewater, 18th ed., American Public Health Association, Washington, DC, 1992, p. 4.43.
[12] B. Ramachandran, H.L. Greene, S. Chatterjee, Appl. Catal. B 8 (1996) 157.
[13] S.K. Agarwal, J.J. Spivey, D.E. Tevault, Appl. Catal. B 5 (1995) 389.
[14] H. Shaw, Y. Wang, T.-Ch. Yu, A.E. Cerkanowicz, in: I.&E.C. Symposium on Emerging Technologies in Hazardous Waste Management, in: ACS Symp. Ser., Vol. 495, Am. Chem. Society, Washington, DC, 1992, p. 358.
[15] C.F. Cullis, B.M. Willatt, J. Catal. 56 (1983) 267.
[16] S.H. Oh, P.J. Mitchell, R.M. Siewert, J. Catal. 132 (1991) 287.
[17] W.R. Patterson, C. Kemball, J. Catal. 2 (1963) 465.
[18] G.L. Golodets, Heterogeneous Catalytic Reactions Involving Molecular Oxygen, Elsevier, Amsterdam, 1983.
[19] R.F. Hicks, H. Qi, M.L. Young, R.G. Lee, J. Catal. 122 (1990) 280.
[20] J.E. Germain, Catalytic Conversion of Hydrocarbons, Academic Press, New York, 1969.
[21] J.E. Germain, Intra-Sci. Chem. Rep. 6 (1972) 101.